Structure, Vol. 12, 1823–1832, October, 2004, ©2004 Elsevier Ltd. All rights reserved. DOI 10.1016/j.str.2004.08.001

Structural Insights into DNA Polymerase β Deterrents for Misincorporation Support an Induced-Fit Mechanism for Fidelity

Joseph M. Krahn, William A. Beard, and Samuel H. Wilson*
Laboratory of Structural Biology
National Institute of Environmental Health Sciences
National Institutes of Health
P.O. Box 12233
Research Triangle Park, North Carolina 27709

Summary

DNA polymerases generally select the correct nucleotide from a pool of structurally similar molecules to preserve Watson-Crick base-pairing rules. We report the structure of DNA polymerase β with DNA mismatches situated in the polymerase active site. This was achieved by using nicked product DNA that traps the mispair (template-primer, A-C or T-C) in the nascent base pair binding pocket. The structure of each mispair complex indicates that the bases do not form hydrogen bonds with one another, but form a staggered arrangement where the bases of the mispair partially overlap. This prevents closure/opening of the N subdomain that is believed to be required for catalytic cycling. The partially open conformation of the N subdomain results in distinct hydrogen bonding networks that are unique for each mispair. These structures define diverse molecular aspects of misinsertion that are consistent with the induced-fit model for substrate specificity.

Introduction

DNA replication and repair synthesis requires that polymerases efficiently incorporate deoxynucleoside triphosphates that preserve Watson-Crick base-pairing rules. The ability to select the correct nucleoside triphosphate (dNTP) from a pool of structurally similar molecules is dependent on the identity of the polymerase. The fidelity of DNA synthesis is primarily coupled to the efficiency with which the polymerase inserts a correct but not incorrect nucleotide (Beard et al., 2002a). This is because most DNA polymerases, independent of their fidelity, insert incorrect nucleotides with similar efficiencies, while correct insertion efficiencies vary widely. Accordingly, the strategies utilized by a specific DNA polymerase to discriminate against incorrect nucleotide insertion may be generally applicable to all polymerases (Beard and Wilson, 2003). In general, DNA polymerases discriminate against noncomplementary, incorrect nucleotides by binding them more weakly and inserting them more slowly than the complementary, correct dNTP. Following nucleotide misincorporation, fidelity may be enhanced by a proofreading exonuclease and/or discouraging further extension of the mismatch. The contribution of each of these steps toward enhancing fidelity varies among DNA polymerases.

Crystallographic structures have been solved for various DNA polymerases in a variety of liganded states. In many instances, these structures have identified molecular interactions that are involved in DNA binding and/or binding of the correct dNTP (Ding et al., 1998; Doublié et al., 1998; Eom et al., 1996; Franklin et al., 2001; Huang et al., 1998; Johnson et al., 2003; Kiefer et al., 1998; Li et al., 1998; Ling et al., 2001; Pelletier et al., 1994; Sawaya et al., 1997). The structures of DNA polymerases derived from diverse sources indicate that they have a modular domain organization. The polymerase domain is typically composed of three functionally distinct subdomains. The catalytic subdomain coordinates two divalent metal cations that assist the nucleotidyl transferase reaction. The other subdomains have principal roles in duplex DNA and nascent base pair (dNTP and templating nucleotide) binding and are spatially situated on opposite sides of the catalytic subdomain. These subdomains are referred to as C (*c*atalytic), D (*d*uplex DNA binding), and N subdomains (*n*ascent base pair binding) to highlight their intrinsic function (Beard et al., 2002b). These would correspond to the palm, thumb, and fingers subdomains, respectively, according to the nomenclature that utilizes the architectural analogy to a right hand (Ollis et al., 1985). Comparison of DNA polymerase structures bound to DNA with those that include an incoming complementary dNTP reveals that the N subdomain repositions itself to "sandwich" the nascent base pair between the growing DNA terminus and the polymerase (Beard and Wilson, 2003). In addition to the polymerase domain, DNA polymerases often have an accessory domain that contributes a complementary enzymatic activity necessary for the enzyme to fulfill its biological task.

DNA polymerase-imposed constraints during nucleotide discrimination have remained poorly understood, in part due to a lack of structural information for polymerases containing mismatched base pairs in their active site. A structural mechanism by which a mismatched incoming nucleotide is averted from binding and catalytic activation is a prerequisite to a detailed molecular understanding of discrimination. This will require a structural description of polymerase-substrate interactions with mismatched base pairs in the confines of the polymerase active site.

DNA polymerase β (pol β) is a DNA repair enzyme that has a key role in the base excision repair pathway. Because of its small size (39 kDa), simple organization (lacks a proofreading exonuclease activity), and the many structural, kinetic, and mechanistic features it shares with other polymerases, it is an ideal model system for structural studies. More importantly, several structures of pol β with nicked, gapped, nongapped, and blunt-end DNA have been determined with or without an incoming dNTP situated in the active site (Arndt et al., 2001; Pelletier et al., 1994, 1996a, 1996b; Sawaya et al., 1997). These structures serve as reference models for

*Correspondence: wilson5@niehs.nih.gov

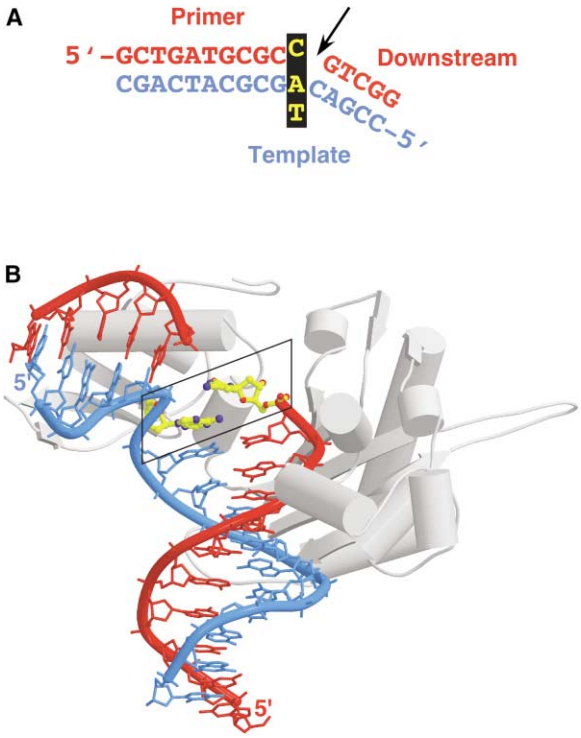

Figure 1. DNA Sequence and Conformation of Mismatches in the DNA Polymerase β Active Site

(A) Primer and downstream oligonucleotides (red) were annealed to template DNA (blue) to generate a nick (arrow). At the nick, the 3′-primer terminus, C, is situated opposite A or T, resulting in an A-C or a T-C mispair (black box). The 5′ end of the primer and template oligonucleotides is indicated.

(B) The global conformation of the polymerase domain (gray) of DNA polymerase β bound to DNA with a terminal A-C mismatch (boxed yellow base pair) situated in the active site. The 8 kDa amino-terminal lyase domain is omitted for clarity. The strategy to trap a mispair at the pol β active site utilized nicked DNA. As shown previously, pol β binds to nicked DNA with the 3′-primer terminus at the "incoming nucleotide" binding pocket (Sawaya et al., 1997). Additionally, artificially producing the mispair through annealing of appropriate oligonucleotides circumvented hydrolysis of incorrect incoming nucleoside triphosphates observed previously (Krahn et al., 2003) and assured full occupancy of the dNTP binding pocket, which has a low affinity for incorrect nucleotides (Ahn et al., 1998; Beard et al., 2004). Figures were created in Molscript (Kraulis, 1991) and rendered with Raster3D (Merritt and Bacon, 1997).

identifying unique interactions that are expected when an incorrect dNTP binds.

Results

Structure Determination

DNA substrates (Figure 1A) and crystallization conditions were designed to be similar to those used in previous crystal structures of pol β with nicked or gapped DNA substrates (Sawaya et al., 1997). These conditions produced similar monoclinic crystals that are compatible with a range of enzyme conformations. Two binary complexes with nicked DNA were obtained. In these situations, the mismatch (template-primer, dA-dC and dT-dC; referred to as NAC and NTC, respectively) is located at the nick. Critically, since the annealed oligonucleotides result in nicked DNA, the mispaired primer terminus binds in the polymerase active site (Figure 1B). They were pursued as a means to ensure full occupancy of the mismatched nucleotide in the incoming dNTP binding site, since the binding affinity for an incorrect nucleotide is much lower than it is for the complementary nucleotide (Ahn et al., 1998; Beard et al., 2004). In contrast, the DNA binding affinity is not significantly perturbed by the introduction of mismatches at the primer terminus (Beard et al., 2004).

Novel Polymerase dNTP Binding Conformation

The pol β mismatch structures illustrate a similar and unique binding mode for the nucleoside base in the incoming dNTP binding pocket. Rather than pairing through nonstandard hydrogen bonds between the mismatched bases, as observed in structures of duplex DNA with central mismatches (Boulard et al., 1995,1997; Brown et al., 1990; Hunter et al., 1986; Kalnik et al., 1988; Sarma et al., 1987), the primer terminus that is now situated in the dNTP binding pocket forms a staggered, partially overlapping interaction with the template base (Figures 2 and 3). An omit map indicates that the mismatch in the 2 Å NAC structure is well defined (Figure 2A), even though the major groove edge of the cytosine ring exhibits weaker density. This was more pronounced in the lower-resolution NTC structure (Figure 2B). The staggered conformation of mispaired bases has been noted previously in the structure of pol β with an incoming dAMP and templating 8-oxodG (Krahn et al., 2003). The position of the mismatched primer terminus in the dNTP binding pocket deviates significantly from previous observations of the correct nucleotide bound to pol β (Sawaya et al., 1997) (Figure 3A). The Watson-Crick edge of the cytosine in the dNTP binding pocket is hydrogen bonded to amino acid side chains rather than the templating adenine (Figure 4B). The specific side-chain interactions of Arg283 and Tyr271 in the mismatch structures differ significantly from those previously observed in the pol β ternary complex with a correct incoming dNTP (Pelletier et al., 1994; Sawaya et al., 1997). These residues stabilize the binding pocket through hydrogen bonds with the n-1 (i.e., template-primer terminus) base pair (Figure 4A). In contrast, the side-chain conformations observed here not only stabilize the observed staggered-base conformation, but also are sterically incompatible with a Watson-Crick base pair in the binding pocket. In the lower-resolution NTC structure, the hydrogen bonding between pol β and the cytosine base in the dNTP binding pocket is more limited (Figure 4C).

Another feature common to the mismatch structures is the presence of a single magnesium ion. The presence of a metal site is clearly defined in electron density maps, with octahedral ligand coordination and bond distances of approximately 2 Å. This geometry corresponds well with that expected for Mg^{2+}, which was included in crystallizations. However, the metal has no protein ligands and does not correspond to either of the previously identified catalytic or nucleoside triphosphate metal sites (Figure 5). Instead, the metal is coordinated to a

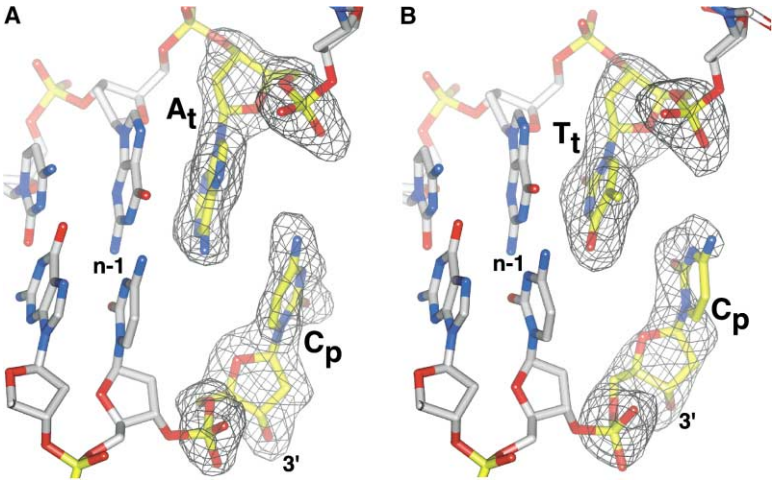

Figure 2. Refined Models of the DNA Polymerase β Active Site DNA Mismatches

F_o-F_c simulated annealing electron density omit maps (gray) contoured at 3.8σ showing electron density corresponding to the A_t-C_p (A) or T_t-C_p (B) mismatches (subscripts refer to whether the nucleotide is situated in the *t*emplate or *p*rimer strands). The densities are superimposed on the refined models of the nicked DNA. The 3′-hydroxyl of the terminal dCMP that is situated in the dNTP binding pocket is indicated. The mismatched base pairs (yellow) are in a staggered conformation precluding direct hydrogen bonding between the bases. The base pair directly upstream of the nascent base pair binding pocket is also indicated (n-1).

nonbridging oxygen on the phosphate of the terminal primer nucleotide and five waters. Furthermore, this metal is 3–3.5 Å away from the two previously identified divalent metal sites and is therefore unlikely to be directly relevant to either dNTP binding or catalysis. The hydrated Mg^{2+} occupies a position corresponding approximately to the dNTP α-phosphate site in the closed pol β conformation and might roughly mimic the β-phosphate position of an intact dNTP in a mismatch structure.

The mismatched nucleotide at the primer terminus is shifted 3–4 Å away from the polymerase catalytic site. This dislocated position permits for hydrogen bond interactions with Arg283 (Figure 4B) and produces three effects that are not consistent with catalysis. First, the α-phosphate is held 2.8 Å away from the catalytic α-phosphate position observed in the active closed ternary complex (Figure 5). Second, the base of the mismatched primer terminus is wedged between the template base and α helix N (Figures 3B and 3C). This prevents α helix N from interacting with the templating base, an event that is thought to be required for catalytic activation. Third, this position disrupts binding of the catalytic magnesium, thus deterring incorporation of the mismatched incoming nucleotide.

N-Subdomain Conformation

The mismatch structures also share similar N-subdomain conformations, which are intermediate between the previously observed closed (ternary complex with correct dNTP) and open (binary pol-DNA) conformations (Figure 6). The closed pol β conformation displays a 25° closure of the N subdomain with respect to the open

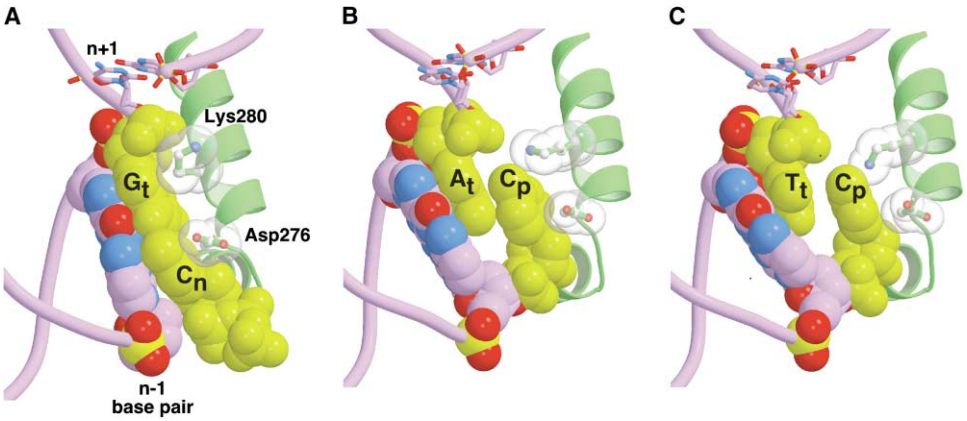

Figure 3. Nascent Base Pair Conformation in the DNA Polymerase β Active Site

(A) A correct base pair (templating guanine, G_t, and incoming ddCTP, C_n; yellow) in the confines of the pol β active site indicates that it is sandwiched between the polymerase (αN, green) and duplex DNA (Sawaya et al., 1997) (Protein Data Bank entry 1BPY). The side chains of Lys280 and Asp276 make van der Waals contact with the bases of the templating and incoming nucleotides, respectively. The primer, downstream, and template strands (lavender) form a one-nucleotide DNA gap, and the nascent and upstream base pairs (n-1) are shown in a Corey-Pauling-Koltun representation. The downstream base pair (n+1) illustrates that the template strand is bent 90° to provide the polymerase an opportunity to assess the geometry of the nascent base pair.

(B) The staggered conformation of the nicked product complex with an A_t-C_p (template-primer) mismatch situated in the active site. The bases of the mismatch partially stack with one another, precluding Watson-Crick hydrogen bonding. Since the product complex results in nicked DNA, the mismatched primer terminus is trapped in the polymerase active site rather than situated in a position (n-1) required to bind an incoming nucleotide.

(C) The staggered conformation of the nicked product complex with a T_t-C_p mismatch situated in the active site.

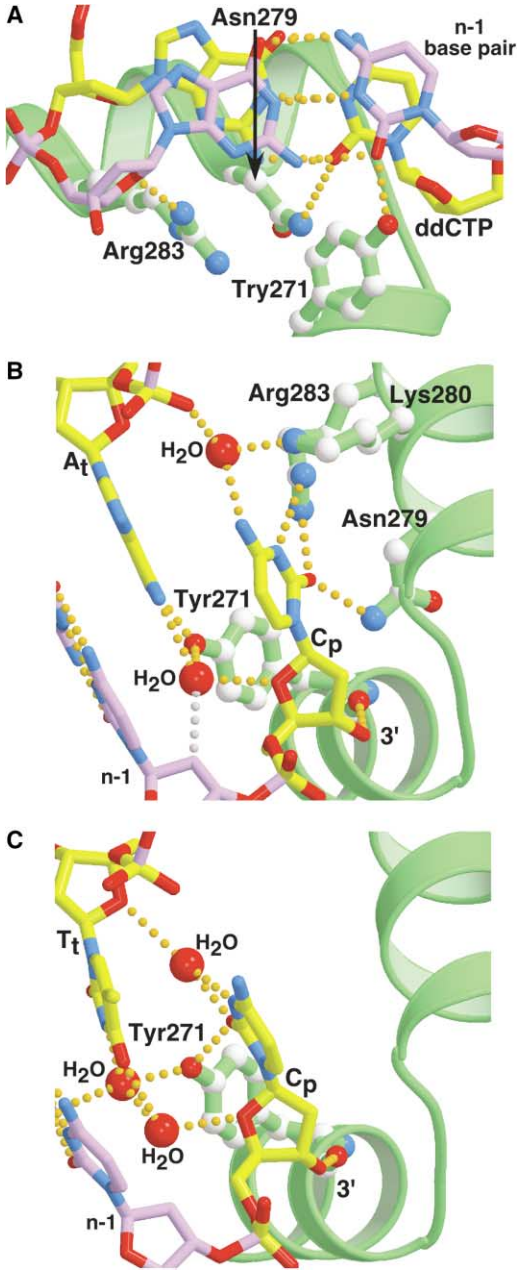

Figure 4. DNA Polymerase β Active Site Hydrogen Bonding Networks

(A) A view down the DNA helix illustrating minor groove hydrogen bonding with a correct base pair (dG-ddCTP, yellow) situated in the pol β (green) active site (Sawaya et al., 1997). The Watson-Crick edges of the bases form standard hydrogen bonds (orange). Tyr271, Asn279, and Arg283 donate hydrogen bonds to the minor groove edge of the primer terminus, incoming nucleotide, and sugar of the n-1 template nucleotide, respectively.

(B) In contrast to when a correct nascent base pair is in the pol β active site, Tyr271 and Arg283 are now observed to hydrogen bond to the template adenine (A_t) and primer cytosine (C_p) bases, respectively, in the staggered conformation of the NAC mismatch (yellow) structure. Two water molecules stabilize the hydrogen-bonding network that includes a weak CH-O hydrogen bond (gray). As with the active conformation with the correct base pair, Asn279 donates a hydrogen bond to the minor groove edge of the cytosine base in the dNTP binding pocket. The 3′-primer terminus is indicated.

(C) The structure of the NTC mismatch complex exhibits a unique hydrogen-bonding network between the polymerase and the mismatch (yellow). In this case, two hydrogen bonds are only observed between the cytosine situated in the dNTP binding pocket and Try271. Arg283 (not shown) is 3.7 Å from O2 of cytosine.

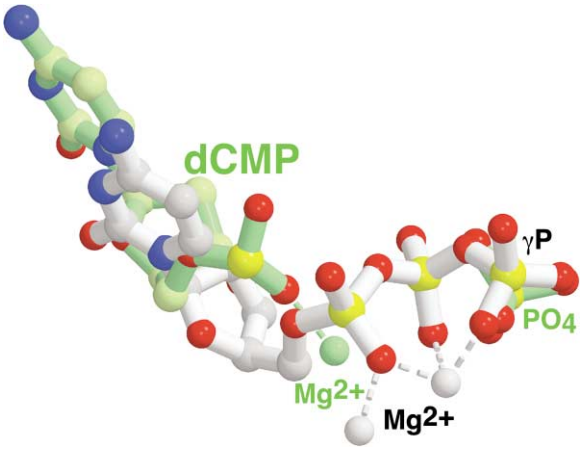

Figure 5. Comparison of Correct and Incorrect Nucleotide Conformations

The conformation of an incoming correct ddCTP (gray) is compared to dCMP (green) from the NAC mismatch structure. These structures were superimposed using the C subdomains (rmsd = 0.65 Å). A single phosphate in the mismatch structure is observed bound to the γP-dNTP binding site. Additionally, a single metal is observed in the mismatch structure that is bound near the αP-dNTP binding site observed in the closed ternary complex. This magnesium ion is coordinated (dashed green line) to a nonbridging oxygen on the phosphate of the terminal primer nucleotide and five water molecules (not shown). The noncomplementary nucleotide at the primer terminus of the mismatch structure has slid into the DNA helix, resulting in a staggered conformation with the templating base. The coordination of the active site metals with the nonbridging phosphate oxygens of the incoming correct nucleotide (gray dashed lines) is also illustrated.

complex, with rotation occurring approximately along the axis of α helix M. The N subdomain of the mismatch structures is closed approximately 7° compared to the open conformation. In contrast, the N subdomain in the structure of pol β with an incoming dAMP and templating 8-oxodG is in a fully open conformation (Krahn et al., 2003). This may be due to the fact that the incoming dAMP and 8-oxodG are displaced toward the center of the DNA helix, providing greater stacking interactions between the mispaired purines thereby wedging the subdomain open.

A major element of catalytic regulation observed in the active closed ternary complex is insertion of Phe272 between the side chains of Asp192 and Arg258, enabling Asp192 to coordinate the two active site Mg^{2+} atoms, thus promoting both substrate binding and catalysis (Sawaya et al., 1997; Vande Berg et al., 2001; Yang et al., 2002) (Figure 7A). Positioning of Phe272 to activate catalysis is coupled to movement of the N subdomain, suggesting a mechanism by which subdomain closure could enable catalysis. Although there is Phe272 backbone movement coupled with the partial closing of the N subdomain, catalytic activation also requires a different

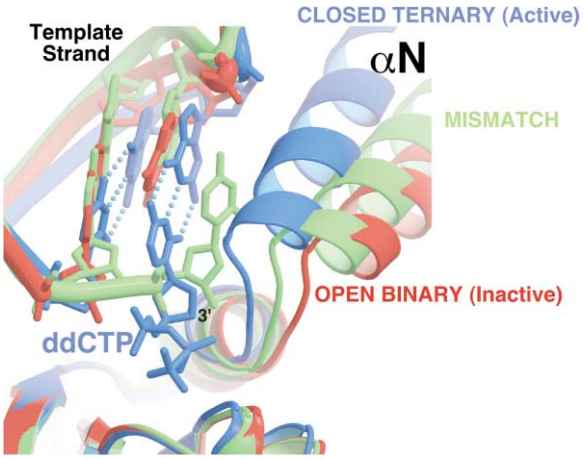

Figure 6. Comparison of Alternate DNA and N-Subdomain Conformations

The conformation of the N subdomain, as monitored by the position of α helix N, for the NAC mismatch structure (green) is in an intermediate position relative to the active closed (blue; Protein Data Bank entry 1BPY) or inactive open (red; Protein Data Bank entry 1BPX) conformations. These structures were superimposed using the C subdomains. The template strand is displaced to a greater extent than that observed for the open binary DNA complex relative to the closed ternary complex. The position of α helix N and the template strand in the open nicked complex (not shown; Protein Data Bank entry 1BPZ) is identical to that illustrated for the open complex.

Phe272 side-chain rotomer. In all pol β structures, the adjacent Tyr271 is in van der Waals contact with Phe272. Tyr271 is in contact with DNA in all three pol β conformations, although specific interactions vary significantly among the three structures. Consequently, Tyr271 appears to function as a direct monitor of the state of bound DNA, with hydrogen bonds formed to the free hydrogen bonding groups in the minor groove of the DNA substrate. Given these observations, it appears that closure of the N subdomain is necessary but not sufficient for catalytic activation, with the activated position specified directly by coupled movements of Tyr271 and Phe272.

Displacement of the Template Strand

Relatively few protein/DNA interactions with the template strand are observed in the product mismatch structures compared to those observed in the closed complex, a feature that is not generally conducive to catalysis. The template strand lacks hydrogen bonds from phosphates n-1, n-2, and n-3 to residues Thr292, Asn294, and Tyr296, respectively, that exist in the closed conformation. An additional hydrogen bond between the n-1 sugar oxygen (O4′) and Arg283 NH1 observed in the closed conformation is mutually exclusive of the interaction between the incorrect cytosine base and Arg283 in the NAC structure (Figures 4A and 4B). This interaction with the n-1 base is particularly important to stabilizing the closed active conformation and template position (Beard et al., 1996, 2002a). The open conformation of pol β with gapped DNA also has reduced contacts with the template strand, although the template strand is not as far removed as it is in the mismatch structures (Figure 6). The template strand displacement is in a direction away from the C and N subdomains, with the n-1 phosphate shifted 4.6 Å compared to the closed conformation and with the n-1 sugar displaced approximately 3 Å. Disruption of the polymerase interactions with the template strand is induced, at least in part, by insertion of the mismatched primer terminus between the template base and α helix N.

Also displaced away from the C subdomain is the 3′-terminal nucleotide of the primer strand (Figure 6). This displacement is accompanied by a sharp deviation from *B*-DNA at the O5′-C5′ bond, with DNA interactions 5′ of this bond essentially unaffected. Movement of this nucleotide away from the C subdomain is probably required for the large displacement of the template strand. Importantly, the structure of the pol β complex bound to nicked DNA with a matched terminus indicates that α helix N and the template strand are in an identical position to that for the open complex with single-nucleotide gapped DNA. In addition, the sugar of the 3′-primer nucleotide in the matched nicked structure overlays with the sugar of the incoming nucleotide in the closed complex. This binding mode results in protection of the primer strand from nucleotide incorporation.

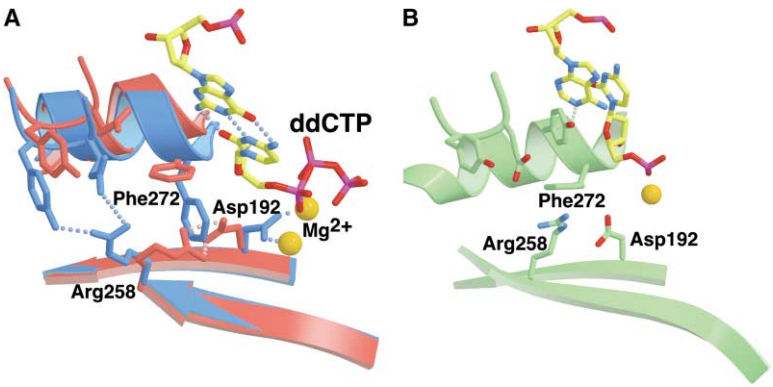

Figure 7. Active Site Catalytic Activation in a Mismatch Structure

(A) Comparison of the conformation of key active-site residues in the open inactive (red; Protein Data Bank entry 1BPX) and closed active (blue; Protein Data Bank entry 1BPY) conformations (Sawaya et al., 1997). In the closed ternary complex structure, Asp192 can form hydrogen bonds with both active site metals (orange). In contrast, Asp192 forms hydrogen bonds with Arg258 in the open conformation. Phe272 insulates Asp192 from Arg258 in the activated conformation by intervening between these side chains when α helix N is in a closed position. The nascent base pair (yellow) in the ternary complex is illustrated.

(B) The conformation of the intermediate mismatch structure (NAC) indicates a transitional position of key active site residues. Although Asp192 does not coordinate the lone active site metal (orange), it also does not interact with Arg258 that is now pointing away from the active site. With the partial closing of α helix N, the backbone of Phe272 approaches an activating position, but the side-chain conformation does not interfere with the potential interaction between Asp192 and Arg258.

HhH Influences DNA Sugar Pucker

The NAC mismatch structure is of sufficiently high resolution to detect significant deviations from ideal *B*-form DNA sugar geometries. Initial refinements restrained the DNA backbone and sugar parameters to an ideal *B*-DNA conformation with C2′-endo sugar puckers. Significant deviations from ideal *B*-form DNA were evident in the refined model and in difference Fourier electron-density maps. A model was refined without *B*-DNA dihedral restraints to better determine deviations from ideality. Pseudorotation values for the resulting sugar puckers indicated that 21 of 32 sugars were in the range for *B*-DNA corresponding to C2′-endo. Two of the remaining eleven (P1 and P10; referring to position, 5′–3′, along the *p*rimer strand) were C2′-exo and C4′-exo, respectively, which can be found in *A*-form DNA (Dickerson and Ng, 2001). The remaining nine sugars demonstrated unrestrained pseudorotations ranging from 90° (O4′-endo) to 141° (C1′-exo). Four of these sugars are found in two adjacent positions at each of the two DNA binding helix-hairpin-helix (HhH) motifs (P8, P9, and D2, D3, where D refers to the *d*ownstream oligonucleotide). The presence of similar deviations at two independent positions suggests that these deviations result directly from binding to the HhH motifs. Two of the remaining five deviant puckers are found at positions where deviations are not unreasonable: at the 90° bend in the template strand (T5) and at the active site (P11). Subsequent refinements excluded sugar pucker dihedral restraints for these residues and used the appropriate C2′-endo restraints for the others.

HhH motifs have been identified in many proteins that bind either single- or double-stranded DNA in a nonsequence-specific manner (Doherty et al., 1996; Mullen and Wilson, 1997; Pelletier et al., 1996a). Binding by the HhH motif occurs primarily at a pair of adjacent backbone phosphates. One phosphate binds to a Na^+ ion at the carboxyl terminus of the first helix, whereas the other binds the amino terminus of the second helix. The HhH binding motif apparently does not bind RNA, yet there are no protein groups near the adjacent sugar C2′ to provide a simple steric exclusion of a 2′-hydroxyl. The 2.0 Å structure of DNA-bound HhH motifs presented here illustrate that DNA specificity may instead be conferred by inducing a sugar pucker that is energetically unfavorable for RNA. The sugar centered between a pair of HhH-bound phosphates straddle the hairpin segment of the HhH motif (Figure 8), conferring steric limitations on the backbone torsion angles. For these sugars, a C1′-exo/O4′-endo pucker is conferred directly by constraining the backbone δ-angle along C4′-C3′. Puckers of the two sugars belonging to the 3′-phosphate at each HhH site also have similar C1′-exo/O4′-endo puckers. A survey of nucleic acid structures indicates that DNA often contains sugars with C1′-exo and O4′-endo sugar puckers (Dickerson and Ng, 2001). This range is significantly less favorable for RNA because it minimizes the distance between the electronegative O2′ and O3′ hydroxyls. The extended range of pseudorotation accessibility to DNA thereby provides a mechanism to discriminate between DNA and RNA that is independent of neighboring nucleic acid structure.

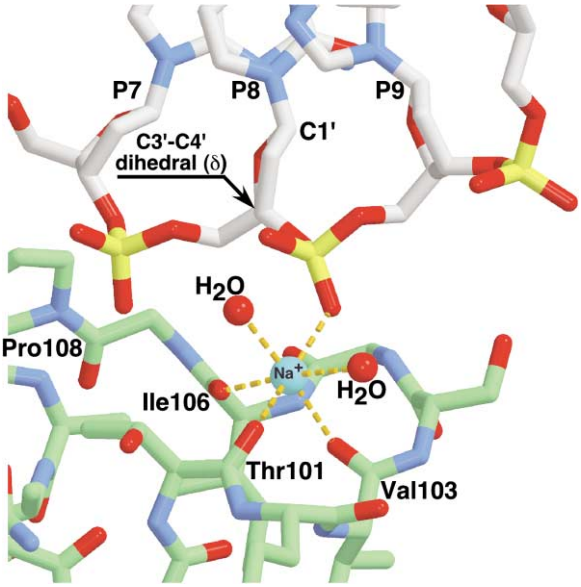

Figure 8. Helix-Hairpin-Helix Motif Recognition of DNA

The 2.0 Å resolution of the NAC mismatch structure was sufficient to determine sugar pucker conformation. The HhH motif binds DNA by utilizing the positive charge of a Na^+ (cyan) bound to the carboxyl terminus of one helix and the amino terminus of the second helix. Although binding primarily involves the phosphate groups, the HhH can produce pucker constraints for the sugars that straddle the HhH. Rigid positioning of the phosphates can constrain the C3′-C4′ dihedral angle. This, in turn, results in a limited range of sugar puckers in the C1′-exo/O4′-endo range. As seen here for the HhH motif that interacts with the primer strand near the 3′ terminus (residues 92–118), C1′ of P8 deviates from planarity in the direction of C1′-exo, but O4′ is also slightly out of plane, toward O4′-endo.

Concluding Remarks and Implications

Comparison of various liganded forms of pol β has illustrated two primary polymerase N-subdomain conformations (Figure 6). The inactive open conformation is common to structures of pol β without DNA (apoenzyme) or complexed with nicked, gapped, or blunt-ended DNA (Pelletier et al., 1996a; Sawaya et al., 1994, 1997). These structures share a similar arrangement of the polymerase subdomains but various positions for the lyase domain. The active closed conformation, observed in a ternary complex with an incoming ddCTP, indicates that the polymerase N subdomain has repositioned itself to sandwich the nascent base pair with the upstream base pair (Pelletier et al., 1994; Sawaya et al., 1997) (Figures 3A and 6). The altered position of the N subdomain is characterized by numerous side-chain and substrate rearrangements. Dynamic simulations of the N-subdomain motion have demonstrated that these local structural transitions do not occur in a single concerted step but in a complex series of events (Yang et al., 2002, 2004; Radhakrishnan and Schlick, 2004). Each of these events results in unique substrate interactions that are not present in the open or closed forms. Accordingly, these interactions may provide distinct opportunities to decipher right from wrong substrates.

Several structural features unique to the mismatch conformation of pol β suggest structural mechanisms that are utilized by DNA polymerases to detect and avert

incorrect nucleotide insertion. The structures of the mismatches in the confines of the pol β active site are consistent with a geometric selection mechanism to discriminate between matched and mismatched base pairs (Echols and Goodman, 1991). This mechanism proposes that the polymerase active site imposes geometric constraints that favor formation of base pairs that comply with these restraints. The ability of an exonuclease-deficient variant of the Klenow fragment of *Escherichia coli* DNA polymerase I (a member of the polymerase A family) to efficiently insert a nonpolar nucleoside isostere of thymidine opposite adenosine (Moran et al., 1997) is consistent with a strict geometric selection. These analogs maintain steric size and shape, even though Watson-Crick and major and minor groove hydrogen bonding groups are absent. However, the ability to insert a nonpolar isostere depends on the identity of the polymerase, indicating that Watson-Crick or minor groove hydrogen bonding may also be critically important in some instances (Morales and Kool, 2000). A kinetic comparison of polymerases exhibiting a wide range of correct nucleotide insertion efficiencies indicates that the incoming nucleotide generally binds with high affinity, but the rate at which it will be inserted depends strongly on the identity of the polymerase (Beard and Wilson, 2003). In contrast, polymerases generally bind incorrect nucleotides with low affinity, indicating that the molecular interactions between the polymerase and wrong incoming nucleotide are compromised. In the NAC structure, many of the hydrogen bonding interactions of the incoming nucleotide observed in the closed polymerase complex are retained in the mismatched structures, albeit with different partners, suggesting that the loss of binding affinity is primarily due to the loss of polymerase and duplex DNA stacking interactions with the nascent base pair (Figure 3).

In addition to the weaker binding affinity for an incorrect dNTP, all DNA polymerases, independent of their fidelity, avert misincorporation by inserting noncomplementary nucleotides more slowly than the correct nucleotide, resulting in low catalytic efficiency (Beard et al., 2002a). The structures of substrate ternary complexes from members of several DNA polymerase families indicate that they exhibit similar active site architectures (geometry of reactive atoms). This architecture is consistent with an in-line nucleophilic substitution reaction for nucleotidyl transfer that proceeds through a pentacoordinated αP transition state. The reaction is assisted by two-metal ions that are coordinated by two universally conserved acidic residues (Steitz et al., 1994). However, since the rate of correct nucleotide insertion can vary over 10^5-fold among polymerases that possess widely divergent fidelities (Beard et al., 2002a; Beard and Wilson, 2003), there are clearly significant active site differences. These differences have been suggested to be electrostatic in nature (Beard and Wilson, 2003). In contrast, the range of misinsertion rates occur over a more narrow range, suggesting that the environment of the reactive atoms with a nascent mispair in the active site may be structurally similar among diverse DNA polymerases. The pol β mismatch structures indicate that the polymerase can exhibit a conformation that is intermediate between an open and closed conformation (Figure 6). In this partially open form, the primer terminus structure is altered relative to that observed in the closed "active" form (Figures 4–6). Since the misinsertion rate would be expected to be very sensitive to the precise positions of the 3′-OH and αP, the distorted primer terminus would strongly diminish the rate of misinsertion. The structures of replicative DNA polymerases (A- and B-family members) and HIV-1 reverse transcriptase indicate that these polymerases contribute functionally important basic side chains of the N subdomain only in the closed conformation. The loss of these stabilizing interactions in a partially opened conformation would also be expected to significantly decrease the rate of incorrect nucleotide insertion.

The mismatch structures indicate that the molecular interactions between the mispair and the polymerase are unique to each mispair. The distinct interactions are partially due to the fact that the hydrogen bonding character of the Watson-Crick edges of the four bases is unique. Whereas Arg283 donates a hydrogen bond to the sugar of the n-1 template nucleotide in the closed polymerase conformation (dG-dCTP) (Figure 4A), it can donate two hydrogen bonds to the mismatched cytosine (N3 and O2) in the partially opened NAC structure (Figure 4B). In contrast, adenine and guanine have a single hydrogen bond acceptor (N1 and O6, respectively), whereas thymine has two (O2 and O4). The major groove hydrogen bond acceptors of guanine (O6) and thymine (O4) are expected to be too far from potential polymerase side-chain interactions. However, major conformational changes in the incoming nucleotide might expose these functional groups for potential polymerase interactions. The unique hydrogen bonding pattern is consistent with the observation that changing the identity of residue 283 through site-directed mutagenesis can dramatically alter the base substitution specificity of pol β (Osheroff et al., 1999). Site-directed mutagenesis of Arg283 had previously identified this residue as critically important in catalysis and fidelity (Ahn et al., 1997; Beard et al., 1996, 2002a).

The structures of DNA mismatches at the template-primer terminus in the confines of an A-family DNA polymerase, *Bacillus* DNA polymerase I fragment, have recently been reported (Johnson and Beese, 2004). These mismatches are situated at the boundary of the nascent base pair binding pocket (i.e., post-insertion site) and, in many instances, are structurally similar to those reported previously in duplex DNA in the absence of protein. In three cases, however (A-A, C-C, and A-G), the primer terminus remained in the nascent base pair binding pocket (i.e., insertion site). In these situations, an aromatic side chain blocks the templating site, and the noncomplementary template base is flipped out of the helix axis into a position referred to as the preinsertion site. The structure of binary DNA complexes of A-family DNA polymerases indicates a similar arrangement of the templating base and aromatic side chain prior to dNTP binding (Kiefer et al., 1998; Li et al., 1998). In contrast, the structure of the binary single-nucleotide gapped DNA complex for pol β indicates that the templating base remains in the DNA helix prior to dNTP binding (see Figure 6 in Beard and Wilson, 2000). Accordingly, geometric constraints imposed by the templating base oc-

Table 1. Crystallographic Statistics

Complex[a]	NAC	NTC
Data Collection		
a (Å)	54.7	54.6
b (Å)	79.7	79.7
c (Å)	54.7	54.6
β (°)	106.8	106.4
d_{min} (Å)	2.0	2.6
R_{merge} (%)[b]	5.9 (18.6)[c]	8.6 (26.2)
Completeness (%)	96.5 (75.1)	98.0 (95.8)
I/σ_I	23.4 (4.4)	13.8 (4.1)
Number of observed reflections	102,046	54,375
Number of unique reflections	29,484	13,572
Refinement		
Rms deviations		
Bond lengths (Å)	0.0091	0.0061
Bond angles (°)	1.39	1.18
R_{work} (%)[d]	17.9	21.2
R_{free} (%)[e]	23.9	28.2
Average B factor (Å^2)		
Protein	22.6	33.2
DNA	21.5	25.4
Ramachandran analysis (%)[f]		
Favored	97.6	95.1
Allowed	100.0	99.7

[a] The binary nicked complexes with the indicated base pair (template-primer terminus) situated in the pol β active site.
[b] $R_{merge} = 100 \times \Sigma_h\Sigma_i|I_{h,i} - I_h|\Sigma_h\Sigma_i I_{h,i}$, where I_h is the mean intensity of symmetry-related reflections $I_{h,i}$.
[c] Numbers in parentheses refer to the highest resolution shell of data (10%).
[d] $R_{work} = 100 \times \Sigma||F_{obs}| - |F_{calc}||/\Sigma|F_{obs}|$.
[e] R_{free} for a 5% subset of reflections.
[f] As determined by MolProbity (Lovell et al., 2003).

cur in part prior to dNTP binding for pol β (X family), whereas these constraints may be imposed subsequent to nucleotide binding for A-family DNA polymerases. The staggered conformation of mismatched nucleotides in the pol β nascent base pair binding pocket is consistent with this proposal.

The dramatically altered protein-DNA interactions and conformations reported for the mismatch structures relative to matched base pairs in the pol β active site are consistent with an induced-fit model for the origin of DNA polymerase fidelity. The induced-fit model states that after initial correct dNTP binding, conformational changes of the ternary complex result in an activated complex where catalytic residues are "aligned" for chemistry. In contrast, the incorrect dNTP results in a poor fit, such that alternate conformational changes result in a suboptimal "activated" complex. Much of the discussion in the literature relative to the induced-fit model has relied on the assumption that a rate-limiting conformational change must limit correct nucleotide insertion (Johnson, 1993; Showalter and Tsai, 2002). Kinetic approaches to measure the first correct nucleotide insertion event have suggested that insertion by A-, B-, and Y-family polymerases is limited by a structurally undefined conformational change (Dahlberg and Benkovic, 1991; Fiala and Suo, 2004; Frey et al., 1995; Washington et al., 2001; Wong et al., 1991). Corresponding evidence for a rate-limiting conformational change is lacking for pol β. Additionally, kinetic (Vande Berg et al., 2001), structural (Arndt et al., 2001), and modeling (Yang et al., 2002) experimental approaches suggest that subdomain motions are too rapid to limit nucleotide insertion. Nevertheless, it has been pointed out that induced fit can alter enzyme specificity even when critical conformational changes are kinetically silent (Post and Ray, 1995), such as when the transition states for correct and incorrect incorporation are unique. Although an induced-fit model reduces enzyme specificity relative to a situation where a unique transition state exists (Post and Ray, 1995), the reduced specificity represents an acceptable compromise for an enzyme such as a DNA polymerase, which must select a different/new substrate (DNA and dNTP) with each catalytic cycle.

Experimental Procedures

Sample Preparation

Wild-type human DNA polymerase β was expressed and purified as described (Beard and Wilson, 1995). The protein was washed four times with several volumes of 20 mM Bis-Tris (pH 7.0) and concentrated to 15 mg ml^{-1}.

DNA substrates consisted of a 16-mer template, a complementary 10-mer primer with an additional noncomplementary 3′ nucleotide (i.e., 11-mer total), and a 5-mer downstream oligonucleotide (Oligos Etc., Redding Center, CT). Proper annealing produces 16 base pair nicked DNA (Figure 1A). The DNA sequence was nearly identical to that used in previous studies (Sawaya et al., 1997) in order to minimize sequence-dependent structural differences. The sequence of the downstream oligonucleotide was 5′-GTCGG-3′, and the 5′ terminus was phosphorylated. The template sequences were 5′-CCGA CAGCGCATCAGC-3′ for the A-C mismatch binary complex (underlined base identifies mismatched base) and 5′-CCGACTGCGCAT CAGC-3′ for T-C mismatch complexes. Primer sequences (11-mer) were 5′-GCTGATGCGCC-3′ for the T-C and A-C binary complexes. Oligonucleotides were dissolved in 20 mM $MgCl_2$, 50 mM Tris/HCl (pH 7.5). Each set of template, primer, and downstream oligonucleotides was mixed in a 1:1:1 ratio and annealed using a PCR thermocycler by heating 10 min at 80°C and cooling to 25°C (1°C min^{-1}), resulting in a 1 mM mixture of nicked duplex DNA. This solution was then mixed with an equal volume of pol β at room temperature. The melting temperature of the 5-mer downstream oligonucleotide is approximately 20°C. Thus, stable association of this short oligonucleotide to the template strand is not likely to occur until addition of pol β. Therefore, a second annealing procedure was applied after addition of pol β to optimize formation of the desired complex. The mixture was warmed to 40°C and cooled gradually to room temperature.

Crystallization and Data Collection

Pol β-DNA complexes were crystallized by sitting drop vapor diffusion versus a reservoir solution of 14%–20% PEG-3350, 350 mM sodium acetate, and 50 mM imidazole (pH 7.5). Drops were incubated at 18°C and streak seeded after 1 day. Crystals grew in approximately 2 to 4 days after seeding, were transferred to cryoprotectant solutions containing artificial mother liquor with 10 mM $MgCl_2$ and 20% ethylene glycol, and then flash frozen to 100 K in a nitrogen stream. Data were collected at 100 K on an R-Axis IV with a Rigaku RU-300 rotating anode generator. Data were integrated and reduced with HKL software (Otwinowski and Minor, 1997).

Structure Determination

The structure of pol β containing nicked DNA with an A-C mismatch was determined by molecular replacement from the structure of pol β complexed with fully complementary nicked DNA (Protein Data Bank accession code 1BPZ). The two crystal structures have similar lattices and are sufficiently isomorphous to determine the molecular-replacement model position by rigid body refinement. The 1BPZ model was modified by substituting oligonucleotide bases with the

appropriate sequence included in the A-C mismatch crystallization. It was refined in CNS (Brünger et al., 1998), first as a single rigid unit against all data to 3.0 Å, then as nine structural subunits (four protein and five oligonucleotide groups) using all data to 2.6 Å, producing a model with an overall R factor of 44%. The model was then subjected to simulated annealing using torsion-angle dynamics with an amplitude maximum likelihood target for all data to 2.0 Å in X-PLOR (Brünger, 1992), producing a working R factor of 33.2% and a free R factor of 39.0%. Subsequent refinement consisted of model building using O (Jones et al., 1991) and refinement in CNS using a maximum likelihood target versus intensities. The working R factor for the final model is 17.9% for all data to 2.0 Å, with a free R factor of 23.9%. Crystallographic data collection and refinement statistics are summarized in Table 1. The NTC structure was determined by a similar procedure using the NAC mismatch structure as a molecular replacement model.

Acknowledgments

We thank L. Pedersen and R. London for critical reading of the manuscript and V. Batra for his assistance in the preparation of Table 1.

Received: March 16, 2004
Revised: July 30, 2004
Accepted: August 4, 2004
Published: October 5, 2004

References

Ahn, J., Werneburg, B.G., and Tsai, M.D. (1997). DNA polymerase β: structure-fidelity relationship from pre-steady-state kinetic analyses of all possible correct and incorrect base pairs for wild type and R283A mutant. Biochemistry *36*, 1100–1107.

Ahn, J., Kraynov, V.S., Zhong, X., Werneburg, B.G., and Tsai, M.-D. (1998). DNA polymerase β: effects of gapped DNA substrates on dNTP specificity, fidelity, processivity and conformational changes. Biochem. J. *331*, 79–87.

Arndt, J.W., Gong, W., Zhong, X., Showalter, A.K., Liu, J., Dunlap, C.A., Lin, Z., Paxson, C., Tsai, M.-D., and Chan, M.K. (2001). Insight into the catalytic mechanism of DNA polymerase β: structures of intermediate complexes. Biochemistry *40*, 5368–5375.

Beard, W.A., and Wilson, S.H. (1995). Purification and domain-mapping of mammalian DNA polymerase β. Methods Enzymol. *262*, 98–107.

Beard, W.A., and Wilson, S.H. (2000). Structural design of a eukaryotic DNA repair polymerase: DNA polymerase β. Mutat. Res. *460*, 231–244.

Beard, W.A., and Wilson, S.H. (2003). Structural insights into the origins of DNA polymerase fidelity. Structure *11*, 489–496.

Beard, W.A., Osheroff, W.P., Prasad, R., Sawaya, M.R., Jaju, M., Wood, T.G., Kraut, J., Kunkel, T.A., and Wilson, S.H. (1996). Enzyme-DNA interactions required for efficient nucleotide incorporation and discrimination in human DNA polymerase β. J. Biol. Chem. *271*, 12141–12144.

Beard, W.A., Shock, D.D., Vande Berg, B.J., and Wilson, S.H. (2002a). Efficiency of correct nucleotide insertion governs DNA polymerase fidelity. J. Biol. Chem. *277*, 47393–47398.

Beard, W.A., Shock, D.D., Yang, X.-P., DeLauder, S.F., and Wilson, S.H. (2002b). Loss of DNA polymerase β stacking interactions with templating purines, but not pyrimidines, alters catalytic efficiency and fidelity. J. Biol. Chem. *277*, 8235–8242.

Beard, W.A., Shock, D.D., and Wilson, S.H. (2004). Influence of DNA structure on DNA polymerase β active site function: extension of mutagenic DNA intermediates. J. Biol. Chem. *279*, 31921–31929.

Boulard, Y., Cognet, J.A.H., Gabarro-Arpa, J., Le Bret, M., Carbonnaux, C., and Fazakerley, G.V. (1995). Solution structure of an oncogenic DNA duplex, the K-*ras* gene and the sequence containing a central C•A or A•G mismatch as a function of pH: Nuclear magnetic resonance and molecular dynamics studies. J. Mol. Biol. *246*, 194–208.

Boulard, Y., Cognet, J.A.H., and Fazakerley, G.V. (1997). Solution structure as a function of pH of two central mismatches, C•T and C•C, in the 29 to 39 K-*ras* gene sequence, by nuclear magnetic resonance and molecular dynamics. J. Mol. Biol. *268*, 331–347.

Brown, T., Leonard, G.A., Booth, E.D., and Kneale, G. (1990). Influence of pH on the conformation and stability of mismatch base-pairs in DNA. J. Mol. Biol. *212*, 437–440.

Brünger, A.T. (1992). X-PLOR, Version 3.1. A System for X-Ray Crystallography and NMR. (New Haven, CT: Yale University Press).

Brünger, A.T., Adams, P.D., Clore, G.M., DeLano, W.L., Gros, P., Grosse-Kunstleve, R.W., Jiang, J.S., Kuszewski, J., Nilges, M., Pannu, N.S., et al. (1998). Crystallography & NMR system: a new software suite for macromolecular structure determination. Acta Crystallogr. D Biol. Crystallogr. *54*, 905–921.

Dahlberg, M.E., and Benkovic, S.J. (1991). Kinetic mechanism of DNA polymerase I (Klenow Fragment): identification of a second conformational change and evaluation of the internal equilibrium constant. Biochemistry *30*, 4835–4843.

Dickerson, R.E., and Ng, H.-L. (2001). DNA structure from A to B. Proc. Natl. Acad. Sci. USA *98*, 6986–6988.

Ding, J., Das, K., Hsiou, Y., Sarafianos, S.G., Clark, A.D., Jr., Jacobo-Molina, A., Tantillo, C., Hughes, S.H., and Arnold, E. (1998). Structure and functional implications of the polymerase active site region in a complex of HIV-1 RT with a double-stranded DNA template-primer and an antibody Fab fragment at 2.8 Å resolution. J. Mol. Biol. *284*, 1095–1111.

Doherty, A.J., Serpell, L.C., and Ponting, C.P. (1996). The helix-hairpin-helix DNA-binding motif: A structural basis for non-sequence-specific recognition of DNA. Nucleic Acids Res. *24*, 2488–2497.

Doublié, S., Tabor, S., Long, A.M., Richardson, C.C., and Ellenberger, T. (1998). Crystal structure of a bacteriophage T7 DNA replication complex at 2.2 Å resolution. Nature *391*, 251–258.

Echols, H., and Goodman, M.F. (1991). Fidelity mechanisms in DNA replication. Annu. Rev. Biochem. *60*, 477–511.

Eom, S.H., Wang, J.M., and Steitz, T.A. (1996). Structure of *Taq* polymerase with DNA at the polymerase active site. Nature *382*, 278–281.

Fiala, K.A., and Suo, Z. (2004). Mechanism of DNA polymerization catalyzed by *Sulfolobus solfataricus* P2 DNA polymerase IV. Biochemistry *43*, 2116–2125.

Franklin, M.C., Wang, J., and Steitz, T.A. (2001). Structure of the replicating complex of a pol α family DNA polymerase. Cell *105*, 657–667.

Frey, M.W., Sowers, L.C., Millar, D.P., and Benkovic, S.J. (1995). The nucleotide analog 2-aminopurine as a spectroscopic probe of nucleotide incorporation by the Klenow fragment of *Escherichia coli* polymerase I and bacteriophage T4 DNA polymerase. Biochemistry *34*, 9185–9192.

Huang, H., Chopra, R., Verdine, G.L., and Harrison, S.C. (1998). Structure of a covalently trapped catalytic complex of HIV-1 reverse transcriptase: Implications for drug resistance. Science *282*, 1669–1675.

Hunter, W.N., Brown, T., Anand, N.N., and Kennard, O. (1986). Structure of an adenine-cytosine base pair in DNA and its implications for mismatch repair. Nature *320*, 552–555.

Johnson, K.A. (1993). Conformational coupling in DNA polymerase fidelity. Annu. Rev. Biochem. *62*, 685–713.

Johnson, S.J., Taylor, J.S., and Beese, L.S. (2003). Processive DNA synthesis observed in a polymerase crystal suggests a mechanism for the prevention of frameshift mutations. Proc. Natl. Acad. Sci. USA *100*, 3895–3900.

Johnson, S.J., and Beese, L.S. (2004). Structures of mismatch replication errors observed in a DNA polymerase. Cell *116*, 803–816.

Jones, T.A., Zou, J.Y., Cowan, S.W., and Kjeldgaard (1991). Improved methods for binding protein models in electron density maps and the location of errors in these models. Acta Crystallogr. A *47*, 110–119.

Kalnik, M.W., Kouchakdjian, M., Li, B.F., Swann, P.F., and Patel, D.J. (1988). Base pair mismatches and carcinogen-modified bases in DNA: An NMR study of A•C and A•O^{4}meT pairing in dodecanucleotide duplexes. Biochemistry *27*, 100–108.

Kiefer, J.R., Mao, C., Braman, J.C., and Beese, L.S. (1998). Visualizing DNA replication in a catalytically active *Bacillus* DNA polymerase crystal. Nature *391*, 304–307.

Krahn, J.M., Beard, W.A., Miller, H., Grollman, A.P., and Wilson, S.H. (2003). Structure of DNA polymerase β with the mutagenic DNA lesion 8-oxodeoxyguanine reveals structural insights into its coding potential. Structure *11*, 121–127.

Kraulis, P. (1991). MOLSCRIPT: a program to produce both detailed and schematic plots of proteins. J. Appl. Crystallogr. *24*, 946–950.

Li, Y., Korolev, S., and Waksman, G. (1998). Crystal structures of open and closed forms of binary and ternary complexes of the large fragment of *Thermus aquaticus* DNA polymerase I: structural basis for nucleotide incorporation. EMBO J. *17*, 7514–7525.

Ling, H., Boudsocq, F., Woodgate, R., and Yang, W. (2001). Crystal structure of a Y-family DNA polymerase in action: a mechanism for error-prone and lesion-bypass replication. Cell *107*, 91–102.

Lovell, S.C., Davis, I.W., Arendall, W.B., III, de Bakker, P.I.W., Word, J.M., Prisant, M.G., Richardson, J.S., and Richardson, D.C. (2003). Structure validation by Cα geometry: ϕ,ψ and Cß deviation. Proteins *50*, 437–450.

Merritt, E.A., and Bacon, D.J. (1997). Raster3D: photorealistic molecular graphics. Methods Enzymol. *277*, 505–524.

Morales, J.C., and Kool, E.T. (2000). Varied molecular interactions at the active sites of several DNA polymerases: Nonpolar nucleoside isoteres as probes. J. Am. Chem. Soc. *122*, 1001–1007.

Moran, S., Ren, R.X.-F., Rumney, S., IV, and Kool, E.T. (1997). Difluorotoluene, a nonpolar isotere for thymine, codes specifically and efficiently for adenine in DNA replication. J. Am. Chem. Soc. *119*, 2056–2057.

Mullen, G.P., and Wilson, S.H. (1997). Repair actvity in DNA polymerases: a structurally conserved helix-hairpin-helix motif in base excison repair enzymes and in DNA polymerase β. In Base Excision Repair in DNA Damage, I.D. Hickson, ed. (Georgetown, TX: Landes Bioscience), pp. 121–135.

Ollis, D.L., Brick, P., Hamlin, R., Xuong, N.G., and Steitz, T.A. (1985). Structure of large fragment of *Escherichia coli* DNA polymerase I complexed with dTMP. Nature *313*, 762–766.

Osheroff, W.P., Beard, W.A., Wilson, S.H., and Kunkel, T.A. (1999). Base substitution specificity of DNA polymerase β depends on interactions in the DNA minor groove. J. Biol. Chem. *274*, 20749–20752.

Otwinowski, Z., and Minor, W. (1997). Processsing of X-ray diffraction data collected in oscillation mode. Methods Enzymol. *276*, 307–326.

Pelletier, H., Sawaya, M.R., Kumar, A., Wilson, S.H., and Kraut, J. (1994). Structures of ternary complexes of rat DNA polymerase β, a DNA template-primer, and ddCTP. Science *264*, 1891–1903.

Pelletier, H., Sawaya, M.R., Wolfle, W., Wilson, S.H., and Kraut, J. (1996a). Crystal structures of human DNA polymerase β complexed with DNA: implications for catalytic mechanism, processivity, and fidelity. Biochemistry *35*, 12742–12761.

Pelletier, H., Sawaya, M.R., Wolfle, W., Wilson, S.J., and Kraut, J. (1996b). A structural basis for metal ion mutagenicity and nucleotide selectivity in human DNA polymerase β. Biochemistry *35*, 12762–12777.

Post, C.B., and Ray, W.J., Jr. (1995). Reexamination of induced fit as a determinant of substrate specificity in enzymatic reactions. Biochemistry *34*, 15881–15885.

Radhakrishnan, R., and Shlick, T. (2004). Orchestration of cooperative events in DNA synthesis and repair mechanism unraveled by transition path sampling of DNA polymerase β's closing. Proc. Natl. Acad. Sci. USA *101*, 5970–5975.

Sarma, M.H., Gupta, G., Sarma, R.H., Bald, R., Engelke, U., Oei, S.L., Gessner, R., and Erdmann, V.A. (1987). DNA structure in which an adenine-cytosine mismatch pair forms an integral part of the double helix. Biochemistry *26*, 7707–7715.

Sawaya, M.R., Pelletier, H., Kumar, A., Wilson, S.H., and Kraut, J. (1994). Crystal structure of rat DNA polymerase β: Evidence for a common polymerase mechanism. Science *264*, 1930–1935.

Sawaya, M.R., Prasad, P., Wilson, S.H., Kraut, J., and Pelletier, H. (1997). Crystal structures of human DNA polymerase β complexed with gapped and nicked DNA: evidence for an induced fit mechanism. Biochemistry *36*, 11205–11215.

Showalter, A.K., and Tsai, M.-D. (2002). A reexamination of the nucleotide incorporation fidelity of DNA polymerases. Biochemistry *41*, 10571–10576.

Steitz, T.A., Smerdon, S.J., Jager, J., and Joyce, C.M. (1994). A unified polymerase mechanism for nonhomologous DNA and RNA polymerases. Science *266*, 2022–2025.

Vande Berg, B.J., Beard, W.A., and Wilson, S.H. (2001). DNA structure and aspartate 276 influence nucleotide binding to human DNA polymerase β: implication for the identity of the rate-limiting conformational change. J. Biol. Chem. *276*, 3408–3416.

Washington, M.T., Prakash, L., and Prakash, S. (2001). Yeast DNA polymerase η utilizes an induced-fit mechanism of nucleotide incorporation. Cell *107*, 917–927.

Wong, I., Patel, S.S., and Johnson, K.A. (1991). An induced-fit mechanism for DNA replication fidelity: direct measurement by single-turnover kinetics. Biochemistry *30*, 526–537.

Yang, L., Beard, W.A., Wilson, S.H., Broyde, S., and Schlick, T. (2002). Polymerase β simulations suggest that Arg258 rotation is a slow step rather than large subdomain motions *per se*. J. Mol. Biol. *317*, 679–699.

Yang, L., Beard, W.A., Wilson, S.H., Broyde, S., and Schlick, T. (2004). The highly organized but pliant active-site of DNA polymerase β: compensatory interaction mechanisms in mutant enzymes by dynamic simulations and energy analyses. Biophys. J. *86*, 3392–3408.

Accession Numbers

Coordinates and structure factors for the NAC and NTC complexes have been deposited in the Protein Data Bank under accession codes 1TV9 and 1TVA, respectively.